

# Non-collinear magnetism in iron at high pressures

R. E. Cohen

*Geophysical Laboratory, Carnegie Institution of Washington  
5251 Broad Branch Rd., N.W., Washington, D.C. 20015*

---

## Abstract

Using a first principles based, magnetic tight-binding total energy model, the magnetization energy and moments are computed for various ordered spin configurations in the high pressure polymorphs of iron (fcc, or  $\gamma$ -Fe, and hcp, or  $\epsilon$ -Fe), as well ferromagnetic bcc iron ( $\alpha$ -Fe). For hcp, a non-collinear, antiferromagnetic, spin configuration that minimizes unfavorable ferromagnetic nearest neighbor ordering is the lowest energy state and is more stable than non-magnetic  $\epsilon$  iron up to about 75 GPa. Accounting for non-collinear magnetism yields better agreement with the experimental equation of state, in contrast to the non-magnetic equation of state, which is in poor agreement with experiment below 50 GPa.

*Key words:* electronic structure, iron, Fe, high-pressure, magnetism, tight-binding  
*PACS:* 71.55.Ak, 64.30.+t

---

## 1 Introduction

Magnetism is known to be important in the phase stability, structure and elastic properties of iron. For example,  $\alpha$ -Fe, the ground state at ambient conditions, would be mechanically unstable if it were not magnetic. Even above the Curie temperature,  $T_c$  there are local magnetic moments in  $\alpha$ -Fe. Face-centered cubic iron (fcc or  $\gamma$ -Fe) has incommensurate magnetic correlations which change rapidly with volume, and give rise to the anti-Invar effect (large thermal expansivity) (Mryasov et al., 1992). The magnetic behavior of hcp iron is important for high pressure materials research, and for interpreting high pressure experiments aimed at understanding the Earth's inner core. Hcp iron is not quenchable to zero pressure, so magnetic studies must be made *in*

---

*Email address:* cohen@gl.ciw.edu (R. E. Cohen).

*situ* at high pressures.  $\epsilon$ -Fe was long thought to be non-magnetic, due to several Mossbauer experiments that showed no hyperfine splitting in  $\epsilon$ -Fe, even down to helium temperatures. However, self-consistent first-principles computations show a magnetic ground state for  $\epsilon$ -Fe which is stable up to about 50 GPa (Steinle-Neumann et al., 1999). Here non-collinear magnetism in  $\epsilon$ -Fe is explored using a magnetic tight-binding model fitted to first-principles calculations.

When magnetic moments are collinear, electrons can be considered to be “spin-up” or “spin-down” in a global sense, i.e. there is a global magnetic quantization direction. This means that one can solve for the spin-up and spin-down electrons separately, and then combine the results to compute the total charge density. When moments are oblique to each other, the spin state is said to be “non-collinear.” In that case the problem does not factorize, and one must diagonalize a Hamiltonian of twice the order of the collinear case. A system can be non-collinear either in response to chemical or thermal disorder, or in order to minimize frustration. Both hcp and fcc lattices are frustrated with respect to antiferromagnetism, in that one cannot order these lattices antiferromagnetically so that all neighbors have opposite spins. This is known to lead to spin-waves and non-collinear magnetism in fcc-Fe. Also, a common example of non-collinear spins occurs on heating bcc-Fe above the Curie point, where the spins disorder dynamically. A comprehensive review of the theory of non-collinear magnetism is given in Sandratskii (1998).

## 2 Method

To study non-collinear magnetism in Fe, a first-principles based non-magnetic tight-binding model (Cohen et al., 1994, 1997; Wasserman et al., 1996) is combined with a model for magnetism (Pickett, 1996; Mukherjee and Cohen, 2001). The Hamiltonian ( $H$ ) of the system is given by,

$$H = H_0 + R^+ H_{collinear} R, \tag{1}$$

where  $H_0$  is the (doubled) non-magnetic Hamiltonian,  $H_{collinear}$  is the collinear magnetic Hamiltonian and  $R$  is the rotation matrix for spin directions, as described below. The overlap matrix  $S$  is unchanged from the non-magnetic non-orthogonal tight-binding model (Cohen et al., 1994, 1997; Wasserman et al., 1996).  $H_0$  was fit to eigenvalues and total energies from an extensive set of non-magnetic Linearized Augmented Plane Wave (LAPW) results within the Generalized Gradient Approximation (GGA) (Perdew et al., 1996) in the bcc, fcc, and hcp structures as functions of pressure and strain, and has been extensively tested (Cohen et al., 1994, 1997; Wasserman et al., 1996).

The magnetic Hamiltonian is twice the size of the original non-magnetic Hamiltonian, with the upper left block being spin-up, the lower right block is spin down, and the off-diagonal blocks are from coupling between up and down spins that give rise to non-collinear magnetic solutions.  $H_0$  is doubled from the original non-magnetic Hamiltonian, with identical diagonal blocks, and zeros on the off-diagonal blocks. The only non-zero elements in the collinear magnetic Hamiltonian  $H_{collinear}$  are the diagonal onsite  $d$  elements. The latter are given by  $-Im_i/2$  for the spin-up block, and  $+Im_i/2$  for the spin-down block, where  $m_i$  is the magnetic moment of the atom  $i$ , and  $I$  is the Stoner parameter, which controls the strength of the exchange splitting (Pickett, 1996).  $R$  is the rotation matrix which depends upon the atomic spin direction with respect to a global reference frame (Uhl et al., 1994). The diagonal of  $H_{mag}$  is spin-up and spin-down, and the off-diagonal bands are the coupling between up and down, which arise from the rotation operation. Similar models have been used previously for incorporating magnetism within a tight-binding approach (You and Heine, 1982; Pickett, 1996; Freyss et al., 1997; Mehl et al., 2001), but the magnetic behavior of  $\epsilon$ -Fe has not been addressed, nor has a first-principles tight-binding model previously been developed that includes constraining fields.

The full spin density matrix is computed, and the constraining fields are computed self-consistently so that spin directions as well as spin moments are self-consistent. The spin-density matrix is given by

$$\rho_{\sigma\sigma'} = \sum_{ij} \psi_{i\sigma} S_{ij} \psi_{j\sigma'} \quad (2)$$

where  $S_{ij}$  is the overlap matrix and  $\psi_{i\sigma}$  are the eigenvectors for atom orbital  $i$  and spin  $\sigma$  in the local coordinate system on each atom. In the local coordinate system the spin on each atom is diagonal and can be represented as up or down. The spin-1/2 rotation matrix elements of  $R$  that rotates from the local coordinate system to the global system with oblique spins is given by

$$R = \begin{pmatrix} R_{\uparrow\uparrow} & R_{\uparrow\downarrow} \\ R_{\downarrow\uparrow} & R_{\downarrow\downarrow} \end{pmatrix} = \begin{pmatrix} \cos \frac{\theta}{2} e^{i\frac{\phi}{2}} & \sin \frac{\theta}{2} e^{-i\frac{\phi}{2}} \\ -\sin \frac{\theta}{2} e^{i\frac{\phi}{2}} & \cos \frac{\theta}{2} e^{-i\frac{\phi}{2}} \end{pmatrix} \quad (3)$$

where  $\theta$  is the polar angle and  $\phi$  is the azimuthal angle. The matrix elements given here are used to build the full rotation matrix; the only non-zero elements are diagonal in atom orbital indices. Without spin-orbit coupling, there is no coupling to absolute directions relative to the crystalline lattice, and only the relative angles between spins are important. Spin-orbit interactions are not included here; their energetic importance is insignificant compared with the exchange energy changes for iron.

The magnetic moments are given by the spin density on each atom summed over the orbitals. The expressions are

$$m = \sqrt{(\rho_{\uparrow\uparrow} - \rho_{\downarrow\downarrow})^2 + 4\rho_{\uparrow\downarrow}\rho_{\downarrow\uparrow}^*} \quad (4)$$

$$\theta = \arccos\left(\frac{\rho_{\uparrow\uparrow} - \rho_{\downarrow\downarrow}}{m}\right) \quad (5)$$

$$\phi = \Im \log \rho_{\uparrow\downarrow}. \quad (6)$$

The magnetic moments are determined self-consistently. One starts with an initial guess, which gives the exchange splittings,  $\pm Im_i/2$ , in the Hamiltonian, find  $H$ , and diagonalize the generalized eigenproblem. States are occupied up to the Fermi level, and the output moment on each atom is found from the weighted eigenvectors and the expressions above. The process is repeated until self-consistency is obtained.

In general the output moment direction, as well as magnitude, will differ from the input. In this way a self-consistent process can be used to find the moment magnitudes and directions that are locally stable. In some cases one wants to compute the energy of a given magnetic structure. In order to guarantee that the output magnetic structure is the desired structure, it is necessary to apply magnetic fields that force the output moments to form the desired structure. Such a procedure has been implemented using a self-consistent procedure with the option to constrain the moments in magnitude and direction (constraining fields contain longitudinal components), or to allow the magnitude to adjust self-consistently, but force the direction to remain as desired (constraining fields are transverse). The procedure used is similar to, but different from, the procedure outlined in Ujfalussy et al. (1999).

The total energy is given by

$$E_{total} = E_b + I \sum m_i^2/4 + \sum \vec{b}_i \cdot \vec{m}_i \quad (7)$$

where  $E_b$  is the band energy (sum of the eigenvalues). There are no additional potential terms; the total energy is obtained from the band structure and moments. The second term in Eq. 7 corrects for double counting of the exchange interaction (Pickett, 1996), and the third term corrects for double counting of the interaction with the applied staggered fields  $\vec{b}_i$ .

The model differs from the conventional Stoner model (Stoner, 1938), in which a ferromagnetic instability is predicted by the inequality  $IN(0) > 1$ , where  $N(0)$  is the non-magnetic density of states at the Fermi level, and the extended Stoner model (Krasko, 1987), in which  $N$  is replaced by the effective density of states  $\tilde{N}(M) = M/\delta\epsilon$ , where  $\delta\epsilon$  is the exchange splitting, in that

our model allows for different hybridization depending on magnetic state, accounting thereby to the actual magnetic structure, i.e. whether the system will be ferromagnetic, antiferromagnetic, or non-collinear.

### 3 Results and Discussion

#### 3.1 *bcc*

The model is in good agreement with previous self-consistent calculations for  $\alpha$ -Fe, especially when a volume dependent  $I$  is used (Mukherjee and Cohen, 2001). The lowest energy state for  $\alpha$ -Fe for the model at ambient and at higher pressures is ferromagnetic, in agreement with the first principles LAPW self-consistent calculations (Stixrude et al., 1994). Moreover, even with a single value of volume independent  $I$  the model calculation describes well the pressure dependence of the magnetic moment and the magnetization energy. As pressure is increased the magnetization energy decreases smoothly (Fig. 1). The value of  $I$  needed for quantitative agreement is almost constant (around 1 eV) for larger atomic volumes or lower pressures but increases for higher pressures. This is consistent with the increase in the exchange interaction at higher pressures noted previously (Asada and Terakura, 1992). Even though the exchange interaction increases with pressure, the non-magnetic density of states near the Fermi energy decreases, giving rise to a net reduction in the magnetic moment and magnetization energy, and finally the loss of magnetism at around atomic volume of 40 bohr<sup>3</sup>.

The Stoner parameter  $I$  was adjusted at each volume to give agreement with self-consistent full-potential Linearized Augmented Plane Wave (LAPW) magnetization energies (Steinle-Neumann et al., 1999) for each volume for bcc.  $I$  is expected to increase as the electronic density increases with decreasing atomic volume, similar to what has been seen before for  $\gamma$ -Fe (Krasko, 1987) and  $\alpha$ -Fe (Fig. 1). Fitting the results to a polynomial valid between  $V = 50$  bohr<sup>3</sup> and 90 bohr<sup>3</sup> gives  $I(eV) = 3.4126 - 0.08583V + 0.00103V^2 - 4.166610^{-6}V^3$ .

#### 3.2 *fcc*

$\gamma$ -Fe shows a great richness in non-collinear magnetic structures as volume is varied, and here it is not explored in detail; much study has been done, as reviewed in Sandratskii (1998). The energies and moments for fcc-Fe with spiral spins along (001) and  $\theta = \pi/2$  were determined using eight-atom supercells, allowing calculations for (00 $q$ ) with  $q = 0, \pi/4, \pi/2, 3\pi/4,$  and  $\pi$ . A k-point

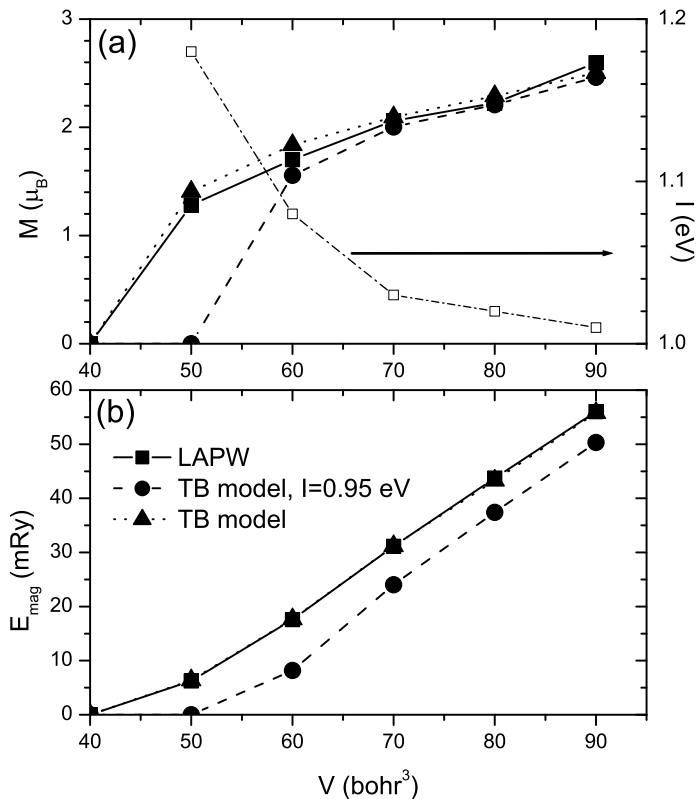


Fig. 1. Magnetization (a) and magnetization energy (b) for bcc iron as functions of volume. The self-consistent LAPW results are from Stixrude et al. (1994). The tight-binding (TB) model results are shown for constant  $I=0.95$  eV, and for varying  $I$ , with  $I$  chosen to best fit the LAPW magnetization energies. The best-fit  $I$  is also shown in (a).

mesh of  $12 \times 12 \times 4$  was used, giving 72 k-points in the irreducible wedge for tetragonal symmetry. For  $\gamma$ -Fe, the complex behavior of magnetic moments and the magnetization energy with increasing pressures and varying spiral spin density wave states is qualitatively reproduced by the model (Figs. 2 and 3) compared with self-consistent calculations (Mryasov et al., 1992; Uhl et al., 1994; Sjöstedt and Nordström, 2002). Quantitatively the results are sensitive to the value of  $I$ , and to get good agreement with self-consistent calculations it seems a smaller  $I$ , about 0.94 eV, is required than derived from bcc-Fe (0.99-1.02 eV for the volumes considered for fcc). In any case there is some variation in self-consistent results for  $\epsilon$ -Fe, due to extreme sensitivity of the magnetic structure to basis set, k-point sampling, etc., due to the small energy scale. Furthermore, the magnetic ground state in  $\gamma$ -Fe is sensitive to the atomic moment approximation (Sjöstedt and Nordström, 2002) in the tight-binding model; that is the moment is really a field that varies with position in the crystal, and is not constant on each atom. Within the atomic moment approximation our results are reasonably consistent with the self-consistent re-

sults. More detailed comparisons with the comprehensive non-collinear LAPW calculations of Sjöstedt and Nordström (2002) including k-point convergence tests are called for, but have not yet been done. In Sjöstedt and Nordström (2002) 4000 k-points were used in the full Brillouin zone, compared to our 4608, which seems comparable. It is more difficult to compare with Mryasov et al. (1992) since a real space multiple scattering approach and a muffin-tin potential approximation was used.

### 3.3 hcp

Previous collinear first principles calculations show stability of an antiferromagnetic state, afmII, in hcp iron (Steinle-Neumann et al., 1999). Moreover, the computed equation of state of afmII greatly improves agreement with the experimental equation of state. An hcp lattice is frustrated for antiferromagnetism; it is not possible to have perfect antiferromagnetic order on it. In the afmII structure each atom has eight antiferromagnetically oriented and four ferromagnetically oriented neighbors, maximizing the antiferromagnetic interactions. In the case of a nearest-neighbor (n.n.) Heisenberg model, which has energy  $E = J_1 \sum_{n.n.} \vec{m}_i \cdot \vec{m}_j$ , the energy is independent of the angle between the moments of one antiferromagnetic pair and another (see Fig.4). If non-neighbourest neighbor interactions are important, or if the Heisenberg model does not completely describe the energetics, the energy might be further lowered if the antiferromagnetic pairs are oblique or perpendicular to each other (i.e.  $\alpha \neq 0$ ).

The collinear afmII structure has 4 atoms per unit cell in space group Pmma (Steinle-Neumann et al., 1999). In order to tile the lattice with the pattern shown in Fig.4 a cell with 8 atoms is obtained with space group A a value of 1.6 was used for  $c/a$  for all of the hcp based calculations here, which is close to the ground state value for the volumes studied here. Tests showed that  $c/a$  does not vary significantly (j.005) with magnetic state. Figure 5 shows the energy versus angle  $\alpha$  for different volumes. In all cases the energy decreases when  $\alpha$  is varied from zero, indicating that the ground state is non-collinear. The most stable state is with  $\alpha=90^\circ$ , which minimizes the local ferromagnetic interactions. Table 1 shows the results of the TB model for hcp Fe with ferromagnetic, admII, and the non-collinear structure with  $\alpha=90^\circ$  (ncl).

The ground state non-collinear total energies of  $\epsilon$ -e were fit to a Vinet equation of state (Vinet et al., 1987) as a function of volume. Table 2 shows the results both using  $K'=4$  and allowing  $K'$  to vary. For non-magnetic Fe,  $K'=4$  is not a bad approximation, but when magnetism is included  $K' > 6$ . The results show that the TB model is in good agreement with the self-consistent

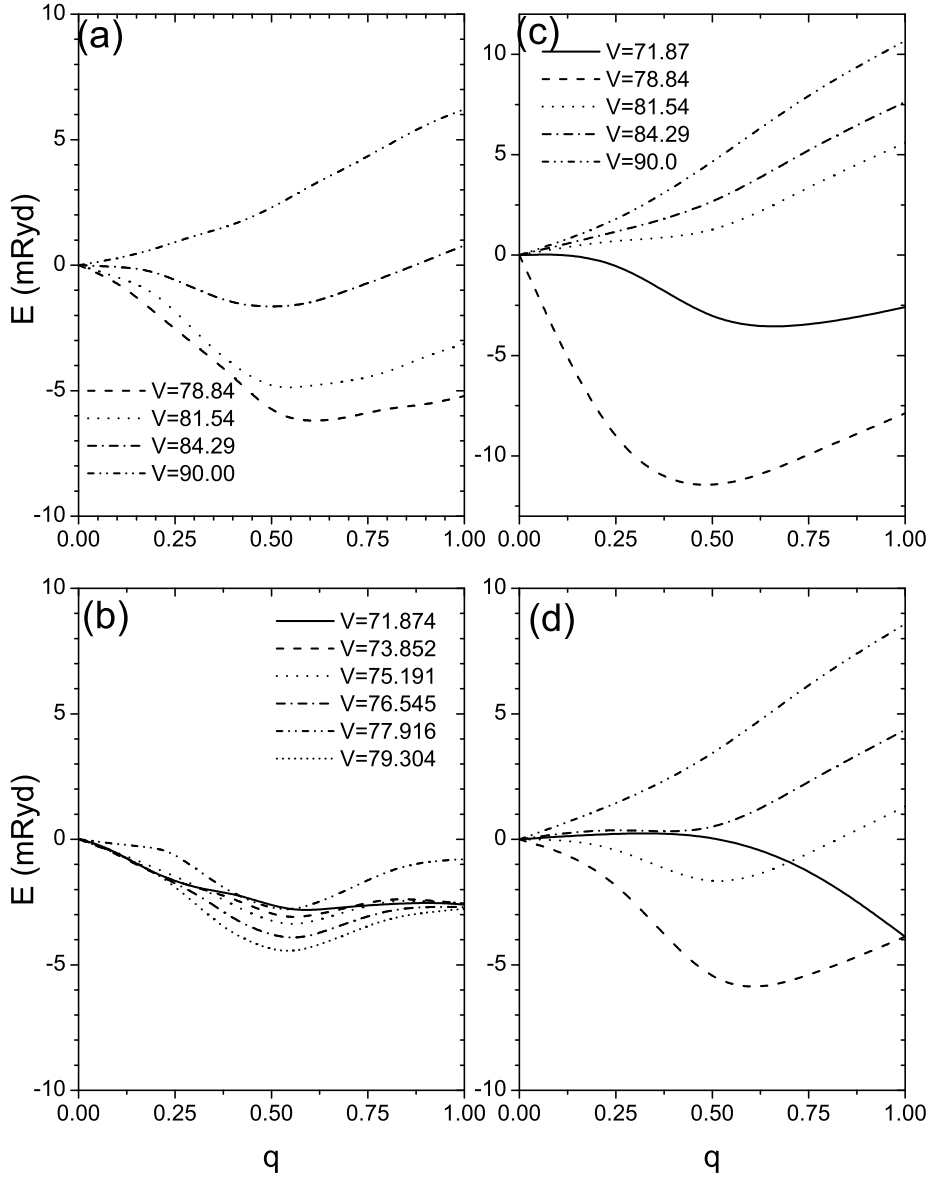


Fig. 2. Variation of magnetization energy versus wavevector for  $\gamma - Fe$  for  $(0,0,q)$ , with  $q$  in units of  $2\pi/a$ , where  $a$  is the lattice constant). Wavevectors  $q = 0$  and  $q = 1$  correspond to ferromagnetic and antiferromagnetic structures, respectively,  $q = 0.5$  is a non-collinear spin state with relative angle between the neighboring spins of  $\pi/2$ . (a) LMTO results from Mryasov et al. (1992). (b) LAPW results from Sjöstedt and Nordström (2002). (c) Results from this study using the best-fit value of  $I$  (1.017, 1.006, 1.003, 1.000, and 0.993 eV for the volumes shown). (d) Results from this study using  $I = 0.94$  eV. The tight-binding results show the correct behavior of ferromagnetic at large volumes and antiferromagnetic at small volumes (high pressures) with a non-collinear transition region. The results of Sjöstedt and Nordström (2002) seem more different than our results and those of Mryasov et al. (1992) than can be explained by the atomic moment approximation. Note that the line dashes and volumes correspond for (a), (c) and (d) but not for (b).



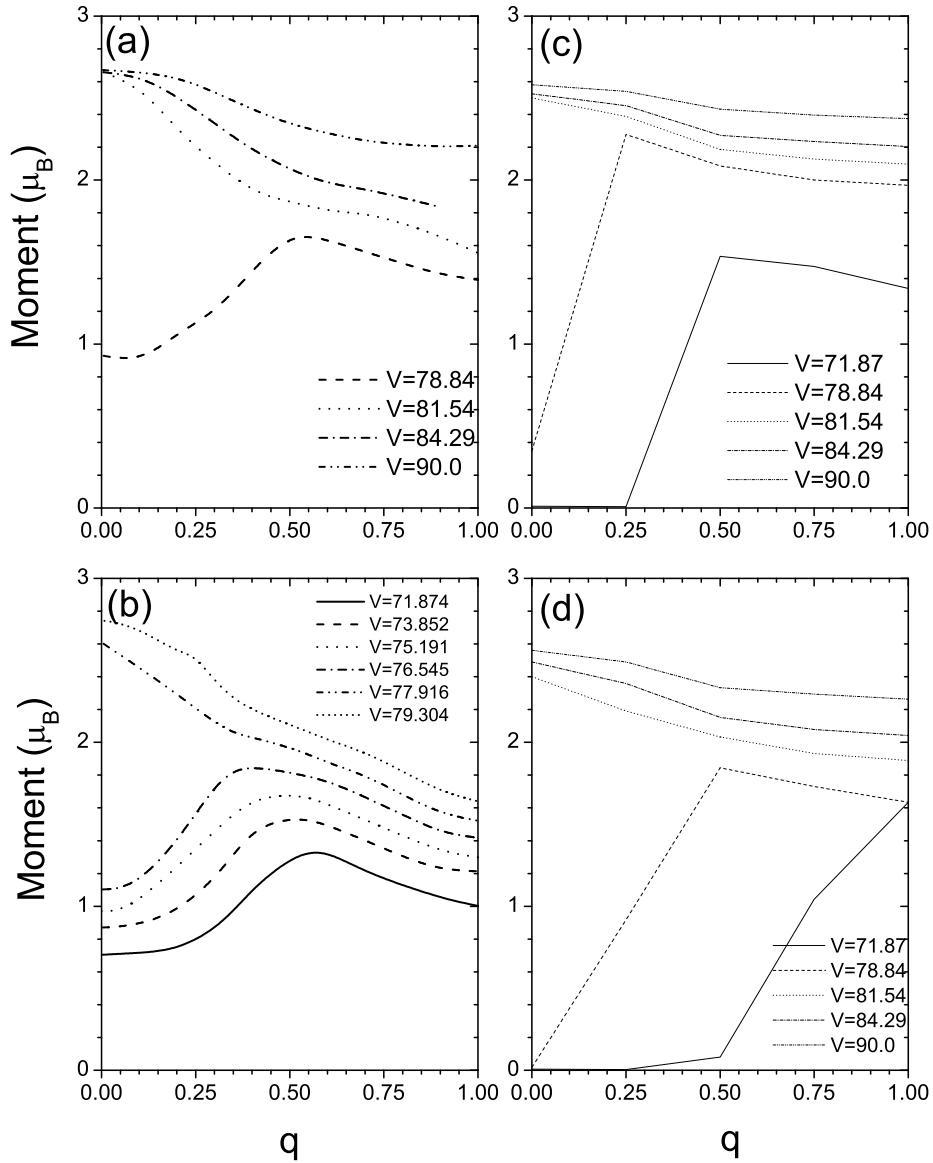


Fig. 3. Variation of moments versus wavevector for  $\gamma - Fe$  for  $(0,0,q)$ . (a) LMTO results from Mryasov et al. (1992). (b) LAPW results from Sjöstedt and Nordström (2002). (c) Results from this study using the best-fit value of  $I$  (1.017, 1.006, 1.003, 1.000, and 0.993 eV for the volumes shown). (d) Results from this study using  $I = 0.94$  eV. Note that the line dashes and volumes correspond for (a), (c) and (d) but not for (b). A high-spin low-spin transition is evident in all cases for ferromagnetic and low- $q$  spin-waves with increasing pressure. The tight-binding model apparently tends to give too small a moment in the low spin regime, but is in generally good agreement.

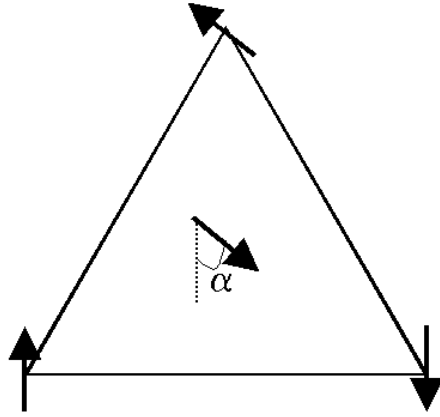


Fig. 4. The motif for an hcp lattice with antiferromagnetic interactions. One pair of antiferromagnetic iron atoms is at an angle  $\alpha$  to another pair. In the Heisenberg model with near-neighbor interactions, the total energy ins independent of  $\alpha$ . The collinear afmII structure is represented by  $\alpha = 0$ .

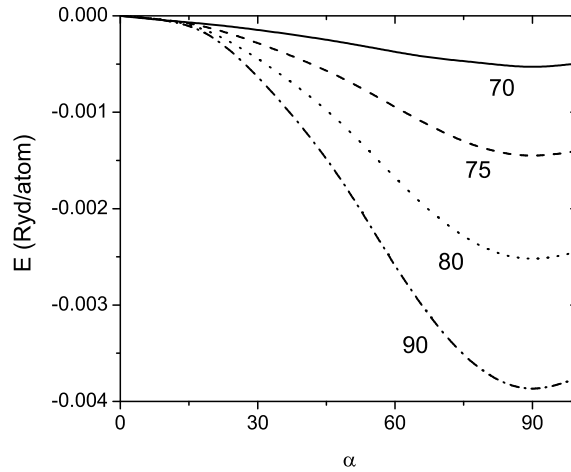


Fig. 5. The motif for an hcp lattice with antiferromagnetic interactions. One pair of antiferromagnetic iron atoms is at an angle  $\alpha$  to another pair. In the Heisenberg model with near-neighbor interactions, the total energy ins independent of  $\alpha$ . The collinear afmII structure is represented by  $\alpha = 0$ .

LAPW computations of Steinle-Neumann et al. (1999). Including magnetism lowers the bulk modulus, and including non-collinear magnetism lowers it further. The resulting equation of state fo ncl is in very good agreement with the experiments (Fig. 6, Table 2) (Jephcoat et al., 1986; Mao et al., 1990). When magnetization is not included the disagreement between the experiment and theory is 75% and 9% for the bulk modulus and the equilibrium volume respectively. Including the afmII structure as the ground state of hcp reduces

Table 1

Magnetization energy (mRy/atom) for different atomic volumes  $V$  (bohr<sup>3</sup>). The value of Stoner parameter  $I$  (eV) for the different volumes is given in the first column. The magnetic moments are given in parenthesis. The non-collinear (ncl) structure is for  $\alpha=90^\circ$

$V$ (au)	$I$ (eV)	Ferro	afmII	ncl
90	1.01	27.1 (2.6)	17.7 (2.28)	21.6 (2.38)
80	1.05	7.2 (2.6)	7.1 (1.79)	9.7 (1.99)
75	1.1	0 (0)	3.1 (1.47)	4.6 (1.67)
70	1.14	0 (0)	0.55 (0.93)	1.1 (1.13)
65	1.19	0 (0)	0.08 (0.33)	0.02 (0.19)

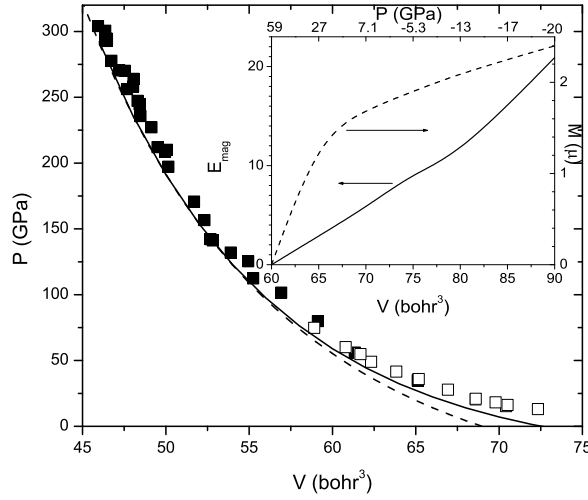


Fig. 6. Equation of state of  $\epsilon$ -Fe. Symbols are experiments from Jephcoat et al. (1986) (open) and Mao et al. (1990) (solid). The solid and the dashed curves are our magnetic and non-collinear NC 1 magnetic theoretical tight-binding results. Inset shows the magnetization energy per atom and moments in NC 1 versus volume. The upper non-linear scale shows the corresponding theoretical pressures.

the disagreement to 25% and 5% for bulk modulus and equilibrium volume (Steinle-Neumann et al., 1999). When the non-collinear spin state energies were used in the equation of state the bulk modulus was within 10% of the experiment.

In spite of theoretical evidence for magnetism in  $\epsilon$ -Fe, and the great improvement in the equation of state when magnetism is included, the experimental situation is unclear. Mössbauer spectroscopy shows no evidence of magnetism in hcp Fe (Taylor et al., 1982, 1991). X-ray absorption spectroscopy also has

Table 2

Comparison of experimental and theoretical values of equilibrium volume ( $V_0$ ) and bulk modulus ( $K_0$ ) for  $\epsilon$ -Fe.

Fe (GGA)	$V_0$ (bohr <sup>3</sup> )	$K_0$ (GPa)	$K'$
Expt(Mao et al., 1990)	75.4	165	
Non-Magnetic (GGA) (Steinle-Neumann et al., 1999)	69.0	292	4.4
Non-Magnetic (this study)	69.1	300	4.0
Non-Magnetic (this study)	68.8	297	4.6
Collinear (afmII) (Steinle-Neumann et al., 1999)	71.2	209	5.2
Collinear (afmII) (this study)	71.3	240	4.0
Collinear (afmII) (this study)	70.1	214	6.3
Non-Collinear (this study)	72.0	227	4.0
Non-Collinear (this study)	70.7	195	6.5

been interpreted to show lack of magnetism (Rueff et al., 1999), but due to the absence of an absolute calibration, and sensitivity of the spectrum to changes in the density of states, the experiments show only that magnetic moments are lower in  $\epsilon$ -Fe than  $\alpha$ -Fe, a result consistent with theory. On the other hand, there is some independent evidence of magnetism from Raman spectroscopy, which shows two peaks (Merkel et al., 2000), instead of the one expected in the hcp structure. The frequencies and splitting of these peaks is predicted well from first-principles calculations for magnetic ordered afmII  $\epsilon$ -Fe (Steinle-Neumann et al., 2003), and the absence of observed splitting in Mössbauer will be explained in a subsequent paper.

Thanks to B. Fultz, A. Goncharov, R. Hemley, A. Jephcoat, I. Mazin, H. Olijnyk, W. Pickett, and G. Steinle-Neumann, L. Stixrude, V. Struzhkin for helpful discussions. S. Mukherjee performed technical assistance. This work was supported by DOE ASCI/ASAP subcontract B341492 to Caltech DOE W-7405-ENG-48 and the National Science Foundation EAR-998002. Computations were performed on the Cray SV1 at the Geophysical Laboratory, supported by NSF grant EAR-9975753 and by the W. M. Keck Foundation.

## References

- Asada, T., Terakura, K., 1992. Cohesive properties of iron obtained by use of the generalized gradient approximation. *Phys. Rev. B* 46, 13599–13602.
- Cohen, R., Mehl, M., Papaconstantopoulos, D., 1994. Tight-binding total energy method for transition and noble metals. *Phys. Rev. B* 50, 14694–14697.
- Cohen, R., Stixrude, L., Wasserman, E., 1997. Tight-binding computations of elastic anisotropy of Fe, Xe, and Si under compression. *Phys. Rev. B* 56, 8575–8589.
- Freyss, M., Stoeffler, D., Dreysse, H., 1997. Interfacial alloying and interfacial coupling in Cr/Fe(001). *Phys. Rev. B* 56, 6047.
- Jephcoat, A. P., Mao, H.-K., Bell, P. M., 1986. Static compression of iron to 78 GPa with rare-gas solids as pressure-transmitting media. *J. Geophys. Res.* 91, 4677–4684.
- Krasko, G. L., 1987. Metamagnetic behavior of fcc iron. *Phys. Rev. B* 36, 8565.
- Mao, H.-K., Wu, Y., Chen, L., Shu, J., Jephcoat, A. P., 1990. Static compression of iron to 300 GPa and Fe<sub>0.8</sub>Ni<sub>0.2</sub> alloy to 260 GPa: Implications for composition of the core. *J. Geophys. Res.* 95, 21737–21742.
- Mehl, M. J., Papaconstantopoulos, D., Mazin, I. I., Bacalis, N., Pickett, W., 2001. Applications of the NRL tight-binding method to magnetic systems. *J. Appl. Phys.* 89, 6880–6882.
- Merkel, S., Goncharov, A., Mao, H., Gillet, P., Hemley, R., 2000. Raman spectroscopy of iron to 152 gigapascals: Implications for Earth’s inner core. *Science* 288, 1626–1629.
- Mryasov, O., Gubanov, V., Liechtenstein, A., 1992. Spiral-spin-density-wave states in fcc iron: Linear-muffin-tin-orbitals band-structure approach. *Phys. Rev. B* 45, 12330–12336.
- Mukherjee, S., Cohen, R. E., 2001. Tight binding based non-collinear spin model and magnetic correlations in Iron. *J. Comp.-Aid. Mat. Des.* 8, 107–115.
- Perdew, J., Burke, K., Ernzerhof, M., 1996. Generalized gradient approximation made simple. *Phys. Rev. Lett.* 77, 3865–3868, correction: *ibid.* 78, 1396 (1997).
- Pickett, W., 1996. Non-collinear magnetic states: From density functional theory to model Hamiltonians. *J. Korean Phys. Soc.* 29, S70.
- Rueff, J. P., Krisch, M., Cai, Y. Q., Kaprolat, A., Hanfland, M., Lorenzen, M., Masciovecchio, C., Verbeni, R., Sette, F., 1999. Magnetic and structural alpha-epsilon phase transition in Fe monitored by x-ray emission spectroscopy. *Phys. Rev. B* 60, 14510–14512.
- Sandratskii, M. L., 1998. Noncollinear magnetism in itinerant-electron systems: theory and applications. *Adv. Phys.* 47, 91–160.
- Sjöstedt, E., Nordström, L., 2002. Noncollinear full-potential studies of  $\epsilon$ -Fe. *Phys. Rev. B* 66, 014447.
- Steinle-Neumann, G., Stixrude, L., Cohen, R., 1999. First-principles elastic constants for the hcp transition metals Fe, Co, and Re at high pressure.

- Phys. Rev. B 60, 791–799.
- Steinle-Neumann, G., Stixrude, L., Cohen, R. E., Kiefer, B., 2003. Evidence of local magnetic order in hcp iron from Raman mode splitting , <http://xxx.lanl.gov/abs/cond-mat/0111487>.
- Stixrude, L., Cohen, R., Singh, D., 1994. Iron at high pressure: Linearized augmented plane wave computations in the generalized gradient approximation. Phys. Rev. B 50, 6442–6445.
- Stoner, E. C., 1938. Collective electron ferromagnetism II. Energy and specific heat. Proc. R. Soc. London, Ser. A 169, 339–371.
- Taylor, R., Cort, G., Willis, J., 1982. Internal magnetic fields in hcp-iron. J. Appl. Phys. 53, 8199–8201.
- Taylor, R., Pasternak, M., Jeanloz, R., 1991. Hysteresis in the high pressure transformation of bcc- to hcp-iron. J. Appl. Phys. 69, 6126–6128.
- Uhl, M., Sandratskii, M. L., Kübler, J., 1994. Spin fluctuations in  $\epsilon$ -Fe and in Fe<sub>3</sub> Pt Invar from local-density-functional calculation. Phys. Rev. B 50, 291–301.
- Ujfalussy, B., Wang, X.-D., Nicholson, D. M. C., Shelton, W. A., Stocks, G. M., 1999. Constrained density functional theory for first principles spin dynamics. J. Appl. Phys. 85, 4824–4826.
- Vinet, P., Ferrante, J., Rose, J., Smith, J., 1987. Compressibility of solids. J. Geophys. Res. 92, 9319–9325.
- Wasserman, E., Stixrude, L., Cohen, R., 1996. Thermal properties of iron at high pressures and temperatures. Phys. Rev. B 53, 8296–8309.
- You, M. V., Heine, V., 1982. Magnetism in transition metals at finite temperatures. I. Computational model. J. Phys. F 12, 177–94.